Biosensors and Bioelectronics 42 (2013) 141–147

Contents lists available at SciVerse ScienceDirect

Biosensors and Bioelectronics

journal homepage: www.elsevier.com/locate/bios

Nonenzymatic biosensor based on Cu_xO nanoparticles deposited on polypyrrole nanowires for improving detection range

Feihong Meng [a,b], Wei Shi [a,*], Yanan Sun [a], Xuan Zhu [b,**], Guisen Wu [a], Changqing Ruan [a], Xin Liu [a], Dongtao Ge [a]

[a] Department of Biomaterials/Biomedical Engineering Research Center, College of Materials, Xiamen University, Xiamen 361005, China
[b] College of Pharmaceutical Science, Xiamen University, Xiamen 361005, China

ARTICLE INFO

Article history:
Received 15 August 2012
Received in revised form
9 October 2012
Accepted 15 October 2012
Available online 22 October 2012

Keywords:
Conducting polymers
Nonenzymatic biosensor
Polypyrrole nanowires
Glucose

ABSTRACT

Cu_xO (CuO and Cu_2O composite) nanoparticles modified polypyrrole (PPy) nanowires were fabricated and used as a biosensor for detecting glucose (GLC). PPy nanowires were prepared through electrodeposition, while Cu_xO nanoparticles were deposited on PPy nanowires by electrodeposition and electrochemical oxidation in situ. The scanning electron microscopy images showed the Cu_xO nanoparticles aligned along the PPy nanowires uniformly and the average size of Cu_xO nanoparticles is about 90 nm. The electrocatalytic activity of Cu_xO/PPy/Au towards GLC was investigated under alkaline conditions using cyclic voltammetry and chronoamperometry. The sensor exhibited a linear range up to 8 mM of GLC, which is more than two times of most of the existing non-enzymatic GLC sensors based on CuO or Cu_2O. The sensitivity of the sensor is 232.22 $\mu AmM^{-1}cm^{-2}$ and detection limit is 6.2 μM (at signal/noise = 3). Moreover, the sensor showed excellent selectivity, reproducibility and stability properties. These excellent performances make Cu_xO/PPy/Au a good nonenzymatic GLC sensor.

1. Introduction

Diabetes, a worldwide chronic disease resulting in metabolic systematic disorder affects more than 220 million people. For these patients, testing of blood glucose (GLC) levels is critical and frequent to avoid blood GLC concentrations exceeding the normal range of 80–120 mg/dL (4.4–6.6 mM) (Wang, 2008). However, there are different interferents that normally coexist with GLC in human blood serum and other samples interfering GLC detection. Accordingly, it is important to develop simple, high sensitivity, good selectivity and stable technologies to detect GLC levels in different fields such as blood, food quality control and pharmaceuticals.

Among the existing approaches to measure GLC concentration, electrochemical techniques, especially amperometric approach have attracted significant attention. The majority of known amperometric biosensors for GLC monitoring focused on two major types, the enzymatic and nonenzymatic GLC sensors. The enzymatic GLC sensors have been widely studied owing to their high sensitivity, selectivity and low detection limit. However, they suffer from poor reproducibility, thermal and chemical instability due to intrinsic nature of enzymes (Tsai et al., 2009). To overcome these drawbacks, many efforts have been made for the amperometric measurements of GLC without using enzyme, including using noble metals, such as Pt (Park et al., 2003; Yuan et al., 2005) and Au (Li et al., 2007; Xia et al., 2011), alloys (Cui et al., 2007; Wang et al., 2008) and metal oxides (Chen et al., 2008; Jiang and Zhang, 2010; Li et al., 2008). Compared with noble metals and alloys, CuO- or Cu_2O- based electrodes exhibited high the catalytic oxidation ability for GLC (Rahman et al., 2010). Especially, the nanostructured CuO and Cu_2O are promising in the development of nonenzymatic glucose sensors because of their highly specific surface area, good electrochemical activity, and the possibility of promoting electron transfer reactions at a lower overpotential (Cherevko and Chung, 2010; Reitz et al., 2008; Zhang et al., 2009a; Zhang et al., 2010; Zhuang et al., 2008). The methods for synthesizing nanostructured CuO and Cu_2O mainly include hydrothermal synthesis in solution (Park et al., 2009; Reitz et al., 2008), sonochemical route (Zhang et al., 2009a, 2009b; Zhang et al., 2010) and heating copper substrates at elevated temperature (Li et al., 2010; Venkatachalam et al., 2009). Although various nanostructured CuO and Cu_2O with different sizes can be obtained by the above methods, the synthesis of CuO or Cu_2O is tedious and often involves surface immobilization.

Besides the kinds of metal or metal oxides, the substrates of nonenzymatic sensors and their spatial structure have been recognized as the important factors influencing the analytical

* Corresponding author. Tel./fax: +86 592 2188502.
** Corresponding author.
E-mail addresses: shiwei@xmu.edu.cn (W. Shi), zhuxuan@xmu.edu.cn (X. Zhu).

0956-5663/$ - see front matter © 2012 Elsevier B.V. All rights reserved.
http://dx.doi.org/10.1016/j.bios.2012.10.051

performance of biosensor. Among the existing materials, nanomaterials synthesized from conducting polymers have been received significant attention for the design of electrochemical biosensors (Lin et al., 2010). Polypyrrole (PPy) nanowire as a typical nanomaterial of conducting polymers is very effective substrate for fabricating biosensors due to its good ordered polymer chain structure with high aspect ratio, small cross dimensions, good electrical properties and excellent biocompatibility (Lin et al., 2010; Jiang et al., 2012). In addition, PPy nanostructure is an excellent material to be used as immobilization matrix for deposition of various nanoparticles (Jeon et al., 2011; Li and Lin, 2007a, 2007b). Therefore, the synergy between PPy nanowires and metal oxides might lead to improve the detection performance of nonenzymatic GLC sensors. However, to our knowledge, nonenzymatic GLC sensors based on metal oxide nanoparticles deposited on nanomaterials of conducting polymers have not been reported so far.

In this paper, Cu_xO (CuO and Cu_2O composite) nanoparticles modified PPy nanowires were successfully prepared through a simple and rapid electrodeposition and electrochemical oxidation in situ. The prepared biosensor integrated advanced properties of nanomaterials PPy and transition metal oxide, and exhibited the excellent detection range, high selectivity, sensitivity and stability. The preparation method and properties of biosensor based on Cu_xO nanoparticles modified PPy nanowires were presented and discussed in detail.

2. Experimental

2.1. Reagents

D-(+)-glucose (GLC), L-ascorbic acid (AA), uric acid (UA), dopamine (DA), D-fructose, mannose, lactose, toluene-4-sulphonic acid sodium salt, pyrrole were purchased from Sinopharm Chemical Reagent Co., Ltd (China). Pyrrole was distilled under vacuum and stored frozen. All other reagents were of analytical grade and were used as received. Deionized water was used for all experiments.

2.2. Instruments

Cyclic voltammetry (CV), electrochemical impedance spectroscopy (EIS) and chronoamperometry were performed on a CHI 660D electrochemical analyzer (Shanghai Chenhua Co, China). A three-electrode system was consisted of a modified Au electrode (3.0 mm diameter) as a working electrode, a reference electrode (SCE saturated KCl) and a counter electrode (Pt wire, 5 mm length, 1 mm diameter). All potentials were referenced to SCE electrode.

X-ray diffraction (XRD) patterns were recorded on an X-ray diffractometer (X'pert PRO, PANalytical), at a scanning rate of $8^\circ\,min^{-1}$ and 2θ range from 30° to 80°. Scanning electron microscopy (SEM) image and energy dispersive spectrometer (EDS) were obtained using SEM (LEO-1530, Germany).

2.3. Preparation of the modified Au electrode

Gold electrode was used as the base electrode for the fabrication of the nonenzymatic biosensor. Before use, the bare Au was polished to a mirror using alumina (under 0.05 μm, diameter) slurries. After each polishing, it was rinsed with doubly distilled water, and then ultrasonicated in ethanol and doubly distilled water for 10 min successively. Finally, it was dried with high purity N_2 and ready for use.

The PPy nanowires were electrodeposited on the surface of Au electrode at a constant potential of 0.8 V for 800 s in a phosphate buffer solution (pH 6.86) containing 0.15 M distilled pyrrole and 0.1 M *p*-toluenesulfonate acid sodium salt (Huang et al., 2010). The PPy nanowires modified electrode was obtained and denoted as PPy/Au.

The Cu nanoparticles were electrochemically deposited on the prepared PPy/Au at a constant potential of −0.60 V in a solution containing 0.1 M KCl and 10 mM $CuCl_2$ for 420 s. Then, they were oxidized by CV scan (Zhi and Qin, 2009). The Cu/PPy/Au was put in 0.1 M NaOH solution and scanned repetitively for 40 cycles under potential range −0.5 to 0.3 V at 50 mVs^{-1} allowing the Cu nanoparticles to be oxidized into copper oxide (Cu_xO) nanoparticles in situ. The obtained Cu_xO/PPy nanocomposite modified Au electrode was denoted as Cu_xO/PPy/Au.

During all experiments, the electrolyte was prepurged with high purity N_2 for 10 min to remove O_2. After each experiment, the electrodes were rinsed several times with water and dried with a flow of N_2. All of the electrochemical experiments were carried out at room temperature in a standard three-electrode system.

2.4. Electrochemical measurements

EIS measurements were carried out in the wide frequency range of 0.1 Hz to 1 MHz under open circuit potential conditions. A 0.1 M KCl solution containing 10 mM $[Fe(CN)_6]^{4-/3-}$ was used as the supporting electrolyte in EIS measurements. The Cu_xO/PPy/Au electrode was evaluated as a GLC sensor by CV and chronoamperometry in 50 mM NaOH. CV measurements were carried out in the potential range of 0.2–0.8 V. Chronoamperometry was carried out at a constant potential of 0.6 V. The background current was allowed to decay to a constant value before GLC sample was added, and then the amperometric curves were obtained after adding the desired amount of GLC into the solution being stirred constantly.

2.5. GLC determination in serum samples

Human blood serum samples were obtained from Zhongshan Hospital of Xiamen University (Xiamen, China). The serum sample (0.5 mL) was added into 10 mL of 50 mM NaOH and a potential of 0.6 V was applied to Cu_xO/PPy/Au electrode to record the current responses. The content of glucose in blood was calculated from working curve.

3. Results and discussion

3.1. Characterization of the Cu_xO/PPy/Au electrode

Surface morphologies of the unmodified PPy nanowires matrix and the Cu_xO/PPy were characterized by SEM. Fig. 1A shows unmodified PPy nanowires, which are clean and relatively smooth in diameter of ~100 nm. The PPy nanowires film has a well-ordered polymer chain structure with very high surface-to-volume ratio, which is beneficial for the attaching of Cu_xO nanoparticles and transport of electrical carriers along one controllable direction. Moreover, small cross dimensions and lots of micropores surrounded by the nanowires could improve incorporation of analytes. Fig. 1B shows the morphology of the Cu_xO/PPy composite, in which Cu_xO nanoparticles are attached on the surface homogeneously and aligned along the PPy nanowires uniformly. The average size of Cu_xO nanoparticles is about 90 nm. The small size and homogeneous distribution of Cu_xO nanoparticles contribute many advantageous properties, such as

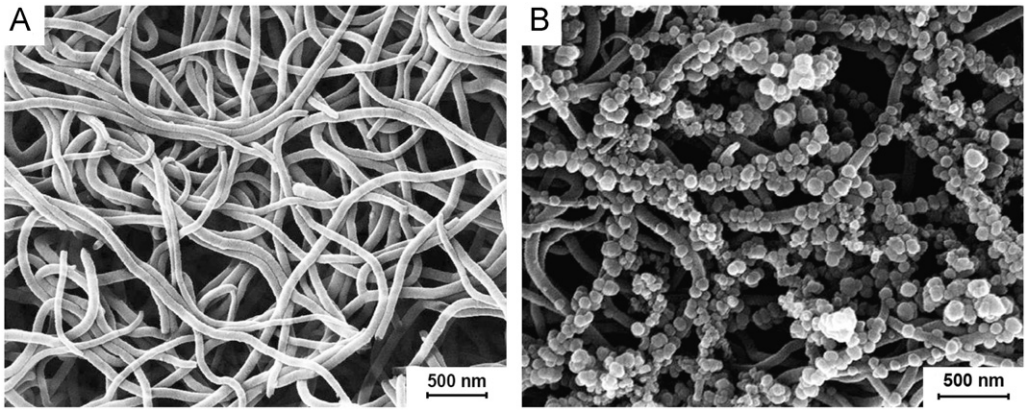

Fig. 1. SEM images of the unmodified PPy nanowires (A) and Cu_xO nanoparticles modified PPy nanowires (B).

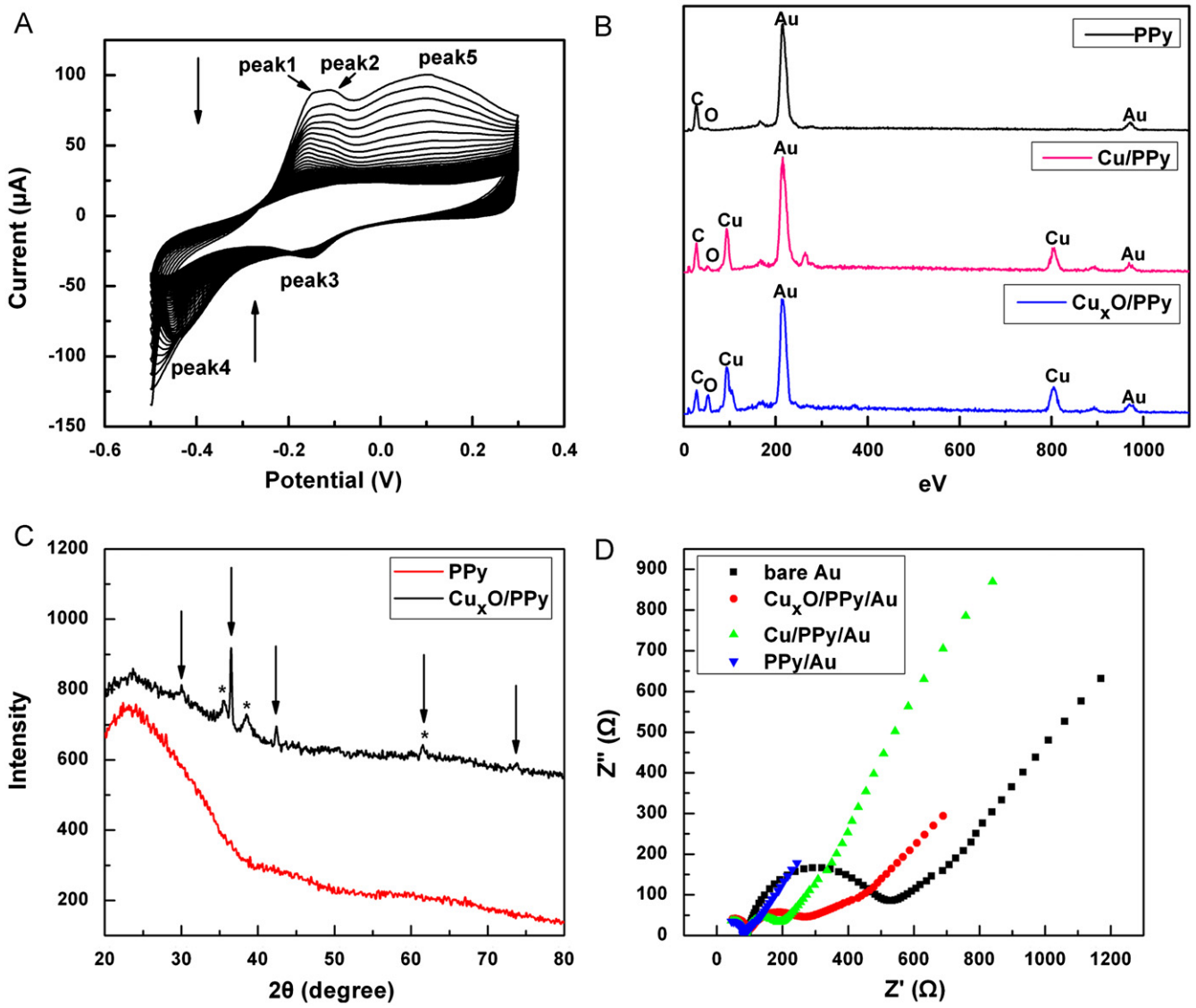

Fig. 2. (A) CV scans of Cu_xO/PPy/Au in 100 mM NaOH at 50 mVs^{-1}. Arrows indicate the progression of the potential scan (scanning range: −0.5 to 0.3 V). (B) EDX spectra of PPy/Au, Cu/PPy/Au and Cu_xO/PPy/Au. (C) XRD spectrum of PPy nanowires and Cu_xO/PPy. Arrows indicate the diffraction peaks of Cu_2O, while stars indicate the diffraction peaks of CuO. (D) EIS of bare Au, PPy/Au, Cu/PPy/Au, Cu_xO/PPy/Au in 0.1 M KCl containing 10 mM $Fe(CN)^{4-/3-}$.

large surface area, good catalysis and large numbers of active sites, which are conducive to an improvement in the stability and sensitivity of Cu_xO/PPy/Au towards GLC oxidation.

Fig. 2A shows the repetitive CV scans of Cu/PPy/Au in 0.1 M NaOH implying oxidation process of Cu nanoparticles. The CV curve displays three anodic peaks (peaks 1, 2 and 5) and two

cathodic peaks (peaks 3 and 4) in the scanning potential range. The anodic peak (peak 5) between 0 and 0.2 V and cathodic peak (peak 3) between −0.2 and −0.1 V are due to the oxidation and reduction of our as-synthesized PPy nanowires, respectively (Ru et al., 2011). The anodic peaks (peak 1 and 2) between −0.2 and 0 V are attribute to the oxidation of Cu_2O and CuOH to CuO, while the cathodic peak (peak 4) between −0.4 and −0.5 V is attribute to the reduction of CuO into Cu_2O and CuOH. Due to the poor conductivities of CuO and Cu_2O, the redox peak currents all decreased with the proceeding of CV scan, indicating that Cu_xO formed successfully. The optimal number of CV scan was 40 according to the catalytic activity for GLC oxidation. The possible mechanism of the electro-chemical oxidation of Cu can be expressed as follows (Zhi and Qin, 2009):

$$Cu + OH^- - e \leftrightarrow CuOH$$

$$2CuOH + OH^- \leftrightarrow Cu_2O + 2H_2O$$

$$CuOH + OH^- - e \rightarrow CuO + H_2O$$

$$Cu_2O + 2OH^- - 2e \leftrightarrow 2CuO + H_2O$$

EDS analysis was used to confirm the elemental compositions at different steps. Fig. 2B shows the EDS spectra of PPy/Au, Cu/PPy/Au and Cu_xO/PPy/Au. Elemental Cu can be observed in the Cu/PPy/Au and Cu_xO/PPy/Au, but absent in the unmodified PPy/Au. This confirms Cu has been successfully deposited onto PPy nanowires. The quantified EDS results of Cu/PPy/Au and Cu_xO/PPy/Au display the atomic ratio of O:Cu before CV increases from 0.06 to 0.8 after CV. This confirms Cu deposited on PPy nanowires has been oxidized into copper oxide by CV. XRD analysis was used to further confirm the composition of Cu_xO deposited on PPy nanowires. Fig. 2C shows the XRD patterns of the Cu_xO/PPy and PPy nanowires. There is no observed diffraction peak in XRD pattern of PPy nanowires, however, there are seven obvious diffraction peaks observed in XRD pattern of Cu_xO/PPy. The diffraction peaks indicated by arrows correspond to Cu_2O (JCPDS 01–077–0199), while those indicated by stars correspond to CuO (JCPDS01–089–5895). No typical peaks are observable for Cu, indicating that the Cu deposited on PPy was completely oxidized into Cu_2O and CuO composite. Cu_xO/PPy/Au fabricated by 120 cycles of CV scan was also determined by XRD. The XRD pattern is similar to that of Cu_xO/PPy/Au fabricated by 40 cycles, indicating that Cu deposited onto PPy nanowires can only be oxidized into CuO and Cu_2O composite, but not into CuO completely in the range of our CV scan.

EIS is a powerful technique for studying the interface properties of electrode surfaces. The Nyquist plots of the bare Au electrode, unmodified PPy/Au, Cu/PPy/Au, and Cu_xO/PPy/Au electrodes in the presence of redox probe $[Fe(CN)_6]^{4-/3-}$ are shown in Fig. 2D. Significant differences in the impedance spectra were observed. The EIS of samples except PPy/Au all included a semicircle portion observed at higher frequency range representing the electron-transfer-limited process and a linear segment at lower frequencies representing the diffusion limited process. The diameter of semicircle portion is equal to the electron transfer resistance (Rct) which reflects conductivity. It is obvious that the bare Au electrode exhibits maximum Rct. However, the EIS of PPy/Au exhibits an almost straight line possibly due to good conductivity of PPy nanowires. In other words, the electron-transfer ability of Au electrode has been greatly improved by depositing PPy nanowires on the surface of Au electrode. The Rct of Cu/PPy/Au was estimated to be 115 Ω. After CV oxidation for Cu/PPy/Au in NaOH, a higher Rct value was found to be 187 Ω. It is mainly because that CuO and Cu_2O are p-type semiconductor with poor conductivity. This result is in consistent with the decreasing redox peak current in Fig. 2A.

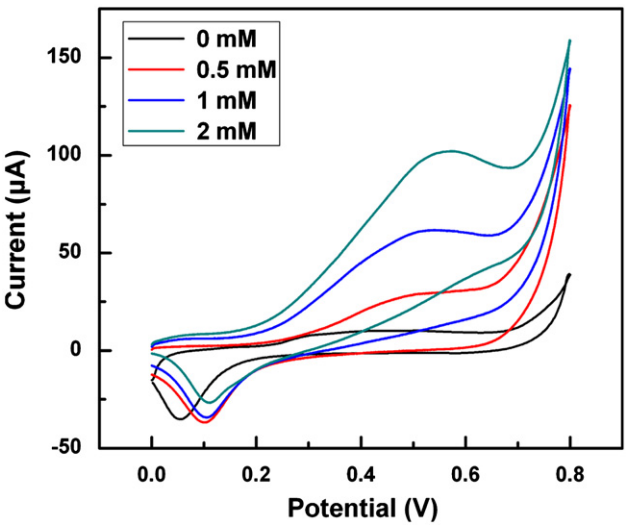

Fig. 3. CV scans of Cu_xO/PPy/Au in 0.1 M NaOH in the absence or presence of 0.5, 1.0, 2.0 mM GLC at 50 mVs^{-1} scanning from 0 to 0.80 V.

In order to verify the electrocatalytic activity of the Cu_xO/PPy/Au toward the oxidation of GLC, CV scan was carried in the absence or presence of GLC in 0.1 M NaOH, as shown in Fig. 3. In the absence of GLC, no oxidation response of GLC can be seen in the potential range from 0 to 0.8 V. Upon adding 0.5 mM GLC, an anodic peak which representing GLC oxidation is observed. Moreover, with the increasing of GLC concentration the anodic peak becomes more obvious and the peak current increases gradually. The oxidation current increases rapidly, starting at about 0.35 V with the appearance of an oxidation peak at around 0.55 V and completing at about 0.7 V. It is obvious that Cu_xO/PPy/Au has good electrocatalytic activity towards the oxidation of GLC.

3.2. Optimization of the sensor

In order to improve the performance of Cu_xO/PPy/Au for GLC oxidation, various factors affecting the response of the sensor were investigated such as the time of depositing Cu nanoparticles, the applied potential and the concentration of NaOH.

Different durations of electrodeposition would result in different amounts of Cu nanoparticles deposited onto PPy/Au, which would eventually generate different catalytic activities towards GLC oxidation. Fig. S1 shows the effect of the deposition time on the electrocatalytic activity of the Cu_xO/PPy/Au towards GLC oxidation by adding GLC in 50 mM NaOH at 0.6 V. The amperometric response increases with the depositing time until 420 s, and then decreases. The current is really low when depositing time is shorter than 300 s or longer than 660 s. Cu nanoparticles could not thoroughly cover PPy nanowires with deposition time shorter than 300 s, however, deposition time longer than 660 s causes the nanoparticles to aggregate into larger particles. The anterior causes insufficient active sites for GLC catalysis and the posterior negates the advantage of larger catalysis area of smaller nanoparticles. The Cu_xO/PPy/Au electrode of depositing time 420 s shows the maximal amperometric response, which is about fivefold that of 300 and 660 s. Hence the optimal time was determined to be 420 s, which generates a sufficient catalysis towards GLC oxidation.

Fig. S2 shows amperometric curves of Cu_xO/PPy/Au in 50 mM NaOH with successive addition of 0.5 mM GLC at different detecting potentials. The amperometric response of GLC oxidation is relatively low when potential is lower than 0.4 V. The response current increases with increasing applied potential, and then

levels off in the range of 0.6–0.7 V. With further increasing of applied potential the side reaction takes place on the electrode, which results in the increase of back current and the inhibition of GLC oxidation (Cherevko and Chung, 2010). Moreover, PPy is easy to be overoxidized in alkaline solution at high potential. The overoxidized PPy has poor electric conductivity and inhibits GLC oxidation. Therefore, 0.6 V was selected as the optimal detecting potential for further amperometric investigations.

It is important to find a suitable detection pH, since the pH would have an important impact on the current and potential of GLC oxidation peaks in cyclic voltammograms. A series of NaOH solutions of different concentrations were used to study the pH effect on GLC oxidation at the Cu_xO/PPy/Au electrode. As shown in Fig. S3, in the range of 10–200 mM, the oxidation current initially increases and then decreases. The higher pH might be conducive to the mutarotation of GLC, which results in the increase of response current. However, too high pH would make GLC isomerizating into fructose and mannose, which results in the decrease of current (Zhang et al., 2009b). The maximal peak current was obtained when NaOH concentration was between 25 and 50 mM. Since the oxidation peak potential correspond to 50 mM is lower than that of 25 mM (Fig. S4), the optimal NaOH concentration was determined as 50 mM.

3.3. Amperometric responses of Cu_xO/PPy/Au towards GLC

Fig. 4A shows the amperometric responses at the applied potential of 0.6 V of Cu_xO/PPy/Au electrode with successive additions of the GLC concentration from 0 to 10.0 mM. The corresponding calibration curve is presented in Fig. 4B. A linear relationship between the current and the concentration was established in the concentration range from 0 to 8 mM (R=0.994), and a sensitivity of 232.22 $\mu A mM^{-1} cm^{-2}$ was obtained from the slope in the linear range. The detection limit is 6.2 μM at a signal-to-noise ratio of 3. The performance of our Cu_xO/PPy/Au sensor is compared with those of other published non-enzymatic GLC sensors based on CuO and Cu_2O in Table 1. As shown in this table, the detection range of most of the existing non-enzymatic GLC sensors based on CuO or Cu_2O was very narrow, which could not cover the concentration range of interest for the determination of glucose in human blood. The linear range of our sensor (0–8 mM GLC) is substantially higher than that of other CuO- and Cu_2O-based sensors, about twice that of the next best sensor (CuO and Cu_2O nanorod composites) (Li et al., 2010). This makes Cu_xO/PPy/Au potential application in practice. Although the sensitivity of our sensor is lower than many CuO- and Cu_2O-based sensors as listed in Table 1, it is higher than that of nonenzymatic GLC sensors based on noble metals such as Pt (Yuan et al., 2005), Au (Li et al., 2007) and alloys Pt–Pb (Cui et al., 2007). The wide linear range, low detection limit and the high sensitive catalytic performance can be ascribed to the nanocomposite nature of Cu_xO based on PPy nanowires. Compared with CuO- or Cu_2O-modified electrode, the Cu_xO (CuO and Cu_2O composite)-modified electrode has a wider linear detection range towards electro-catalytic oxidation of GLC due to the synergic effect of CuO and Cu_2O (Li et al., 2010). Moreover, the PPy nanowires can finely disperse Cu_xO nanoparticles, and the nanostructures Cu_xO nanoparticles can greatly increase the electrocatalytic active areas and promote electron transfer. In addition, the PPy nanowires with large pores can provide larger surface area for GLC molecules to be adsorbed, effectively transfer electrons between the Au and Cu_xO active sites, and high mass transportation rate, which can reduce the amount of oxidation products accumulated on the catalytic sites and prevent the electrode from fouling.

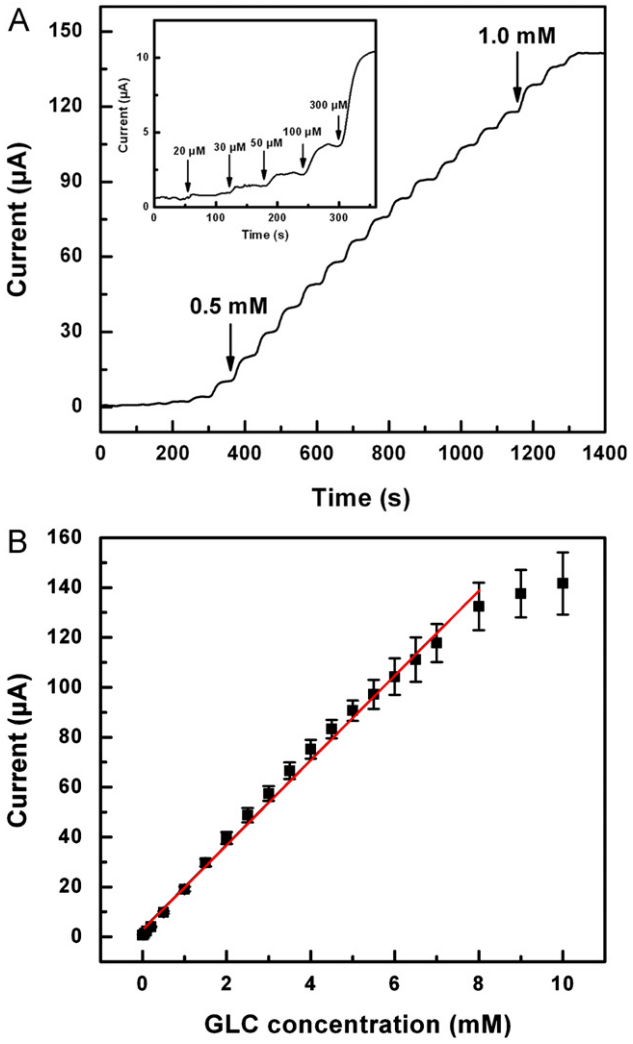

Fig. 4. (A) Current–time responses of Cu_xO/PPy/Au with successive increasing GLC concentration at 0.6 V. The inset shows the magnified view of the current–time response at low concentrations of GLC. (B) The dependence of the current response vs. GLC concentration. Error bars indicate standard deviations for three independent measurements by separately prepared electrodes.

3.4. Selectivity and stability

Anti-interference ability is important in practical use of the biosensors. The oxidizable compounds such as UA, AA and DA are normally coexisted with GLC in human blood serum and other samples. They can be oxidized on the electrode surface and produce interfering electrochemical signals. The physiological GLC level is 4.4–6.6 mM (Wang, 2008) while the other interferents are present at levels as low as 0.1 mM (Safavi et al., 2009; Zhuang et al., 2008). Herein, the amperometric responses of the Cu_xO/PPy/Au towards 2.0 mM GLC and 0.1 mM DA, AA, UA, lactose, mannose and fructose as well as 0.4 mM NaCl were examined in 50 mM NaOH. Fig. S5 shows the interference test of the Cu_xO/PPy/Au in 50 mM NaOH with 2.0 mM GLC and other interferents at 0.5, 0.6 and 0.7 V. When the applied potential is 0.5 V, the selectivity is high and the current response of interferes are negligible. However, associated with the increase of applied potential, the current response of interferes increase. The response currents of GLC, DA, UA, AA, lactose, fructose, mannose and NaCl at 0.6 V are 34, 0.4, 0.3, 1.3, 0.1, 0.1, 0.05 and 0.02 μA, respectively (Fig. S5). This result demonstrates the current interferences are only 0.06–4% as that of GLC. The obtained selectivity

Table 1
Comparison of the performance of as-synthesized Cu_xO/PPy/Au sensor with other published nonenzymatic GLC sensors based on CuO and Cu_2O.

Electrode materials	Operational potential (V)	Sensitivity ($\mu Acm^{-2}mM^{-1}$)	Linear range (up to mM)	Detection limit (μM)	References
Porous cuprous oxide (Cu_2O) microcubes	0.6	−1002	0.5	0.8	Zhang et al., 2009a
CuO nanospheres	0.6	404.5	2.55	1.0	Reitz et al., 2008
Cu_2O–Nafion film	0.4	155.1	0.35	1.3	Zhang et al., 2010
Porous CuO film	0.65	2900	2.5	0.14	Cherevko and Chung, 2010
Cu_2O/MWCNTs nanocomposites	−0.2	9.24×10^4	0.01	0.05	Zhang et al., 2009b
CuO and Cu_2O nanorod composites	0.5	1620	4.0	49	Li et al., 2010
Cu_xO/PPy/Au	0.6	232.22	8.0	6.2	This work

MWCNTs: multi-walled carbon nanotubes.

Table 2
Determination of GLC in human blood serum samples.

Blood serum samples	CLC concentration measured by hospital (mM)	GLC concentration measured by Cu_xO/PPy/Au electrode (mM)	RSD (%)
1	4.5	4.3	2.3
2	5.8	5.6	3.4
3	5.9	5.8	3.1
4	6.5	6.3	2.8

is better than that found for the porous CuO film electrode (Cherevko and Chung, 2010), CuO nanospheres electrode (Reitz et al., 2008) and Cu_2O–Nafion film electrode (Zhang et al., 2010). It should be pointed out that the chloride poisoning as a major problem for most metal or metal oxide nonenzymatic GLC sensors (Song et al., 2005; Sun et al., 2001) was not found in our study. The improved selectivity is due to the synergy of Cu_xO nanoparticles and the alkali medium. For example, DA and AA are easily oxidized when they are added into the alkali medium, however they are unlikely to react with Cu_xO and consequently result in weak signals. As for UA, which is in the highest oxidation state, it is difficult to be oxidized by Cu_xO (Zhang et al., 2009b). Therefore, the selectivity of Cu_xO/PPy/Au for GLC detection is satisfied in the presence of possible interfering reagents.

The stability of Cu_xO/PPy/Au includes operation stability and storage stability. The operation stability was investigated by monitoring current response of Cu_xO/PPy/Au during a long period of 30 min for 5 mM GLC in 50 mM NaOH. There is a loss of only 2.2% in the current response. The storage stability was investigated by measuring its sensitivity under ambient conditions over 10 days. It was found that 96.2% of its original sensitivity was remaining after 10 days. The stability of as-synthesized Cu_xO/PPy/Au sensor is similar with that of Cu_2O–Nafion film electrode (Zhang et al., 2010), but better than that of Cu_2O/MWCNTs nanocomposites electrode (Zhang et al., 2009b) and porous Cu_2O microcubes electrode (Zhang et al., 2009a). A series of repetitive measurements were carried out in 5 mM GLC to determine the repeatability and reproducibility of the sensor. The current responses of one chosen electrode in 5 mM GLC were successively measured five times and yielded a relative standard deviation (RSD) of 1.7%, indicating that the sensor can be used repeatedly for the detection of GLC. To evaluate the reproducibility of the sensor, three individual electrodes are tested independently for the amperometric response of glucose, providing a RSD of 3.4%. This confirmed that the fabrication method was highly reproducible. The long-term stability and good reproducibility of Cu_xO/PPy/Au make it suitable for practical use.

To verify the sensor can be applied in clinical diagnostics, the as-synthesized Cu_xO/PPy/Au electrodes were used to determine GLC concentration of human blood serum. Serum sample (0.5 mL) was added to 10 mL of 50 mM NaOH as testing solution and the testing results are showed in Table 2. Each sample was performed for three times and the detection concentration was the average of the three detection results. The GLC concentrations of the samples are in good agreement with the results provided by Zhongshan Hospital (Xiamen, China).

4. Conclusions

We successfully fabricate a novel nonenzymatic GLC sensor, Cu_xO/PPy/Au, by a simple method. The as-synthesized Cu_xO/PPy/Au electrochemical sensor has a wide linear range up to 8 mM GLC concentration, a low detection limit of 6.2 μM and a high sensitivity of 237.22 $\mu AmM^{-1}cm^{-2}$. These excellent performances including ease of fabrication, high selectivity, sensitivity, especially wide linear range, make Cu_xO/PPy/Au a good amperometric sensor for GLC determination.

Acknowledgments

The authors acknowledge the support from the National Nature Science Foundation of China (Nos. 30500127, 31070845), the Natural Science Foundation of Fujian Province of China (No. 2011J01331) and the Fundamental Research Funds for the Central Universities (No. 2011121001).

Appendix A. Supporting information

Supplementary data associated with this article can be found in the online version at http://dx.doi.org/10.1016/j.bios.2012.10.051.

References

Chen, J., Zhang, W.D., Ye, J.S., 2008. Electrochemistry Communications 10, 1268–1271.
Cherevko, S., Chung, C.H., 2010. Talanta 80, 1371–1377.
Cui, H.F., Ye, J.S., Zhang, W.D., Li, C.M., Luong, J.H.T., Sheu, F.S., 2007. Analytica Chimica Acta 594, 175–183.
Huang, J.Y., Wang, K., Wei, Z.X., 2010. Journal of Materials Chemistry 20, 1117–1121.
Jeon, S.S., Kim, C., Ko, J., Im, S.S., 2011. Journal of Physical Chemistry C 115, 22035–22039.
Jiang, H.R., Zhang, A.F., Sun, Y.N., Ru, X.N., Ge, D.T., Shi, W., 2012. Electrochimica Acta 70, 278–285.
Jiang, L.C., Zhang, W.D., 2010. Biosensors and Bioelectronics 25, 1402–1407.
Li, C.C., Liu, Y.L., Li, L.M., Du, Z.F., Xu, S.J., Zhang, M., Yin, X.M., Wang, T.H., 2008. Talanta 77, 455–459.
Li, C.L., Su, Y., Zhang, S.W., Lv, X.Y., Xia, H.L., Wang, Y.J., 2010. Biosensors and Bioelectronics 26, 903–907.
Li, J., Lin, X.Q., 2007a. Microchemical Journal 87, 41–46.
Li, J., Lin, X.Q., 2007b. Sensors and Actuators B 126, 527–535.

Li, Y., Song, Y.Y., Yang, C., Xia, X.H., 2007. Electrochemistry Communications 9, 981–988.
Lin, M., Cho, M.S., Choe, W.S., Yoo, J.B., Lee, Y., 2010. Biosensors and Bioelectronics 26, 940–945.
Park, J.C., Kim, J., Kwon, H., Song, H., 2009. Advanced Materials 21, 803–807.
Park, S., Chung, T.D., Kim, H.C., 2003. Analytical Chemistry 75, 3046–3049.
Rahman, Md, M., Ahammad, A.J.S., Jin, J.H., Ahn, S.J., Lee, J.J., 2010. Sensors 10, 4855–4886.
Reitz, E., Jia, W.Z., Gentile, M., Wang, Y., Lei, Y., 2008. Eletroanalysis 20, 2482–2486.
Ru, X.N., Shi, W., Huang, X., Cui, X., Ren, B., Ge, D.T., 2011. Electrochimica Acta 56, 9887–9892.
Safavi, A., Maleki, N., Farjami, E., 2009. Biosensors and Bioelectronics 24, 1655–1660.
Song, Y.Y., Zhang, D., Gao, W., Xia, X.H., 2005. Chemistry-a European Journal 11, 2177–2182.
Sun, Y.P., Buck, H., Mallouk, T.E., 2001. Analytical Chemistry 73, 1599–1604.
Tsai, T.W., Heckert, G., Neves, L.F., Tan, Y.Q., Kao, D.Y., Harrison, R.G., Resasco, D.E., Schmidtke, D.W., 2009. Analytical Chemistry 81, 7917–7925.
Venkatachalam, S., Zhu, H.W., Masarapu, C., Hung, K.H., Liu, Z., Suenaga, K., Wei, B.Q., 2009. ACS Nano 3, 2177–2184.
Wang, J., 2008. Chemical Reviews 108, 814–825.
Wang, J.P., Thomas, D.F., Chen, A.C., 2008. Analytical Chemistry 80, 997–1004.
Xia, Y., Huang, W., Zheng, J.F., Niu, Z.J., Li, Z.L., 2011. Biosensors and Bioelectronics 26, 3555–3561.
Yuan, J.H., Wang, K., Xia, X.H., 2005. Advanced Functional Materials 15, 803–809.
Zhang, L., Li, H., Ni, Y.H., Li, J., Liao, K.M., Zhao, G.C., 2009a. Electrochemistry Communications 11, 812–815.
Zhang, L., Ni, Y.H., Li, H., 2010. Microchimica Acta 171, 103–108.
Zhang, X.J., Wang, G.F., Zhang, W., Wei, Y., Fang, B., 2009b. Biosensors and Bioelectronics 24, 3395–3398.
Zhi, L.W., Qin, L.Y., 2009. Sensors and Actuators B 141, 147–153.
Zhuang, Z.J., Su, X.D., Yuan, H.Y., Sun, Q., Xiao, D., Choi, M.M.F., 2008. Analyst 133, 126–132.